IIETA International Information and Engineering Technology Association
Advancing the World of Information and Engineering

Journal Européen des Systèmes Automatisés
Vol. 58, No. 12, December, 2025, pp. 2545-2556
Journal homepage: http://iieta.org/journals/jesa

Modern Control and Applications of Compound DC Motors: Performance, Techniques, and Developments

Husam Jawad Ali[1*], Wafeeqa Abdulrazak Hasan[2], Qahtan A. Jawad[3]

[1] Department of Computer Engineering Techniques, Shatt Al-Arab University College, Basra 61001, Iraq
[2] Department of Electrical Engineering Techniques, Basrah Engineering Technical College, Southern Technical University, Basrah 61001, Iraq
[3] Department of Mechanical Engineering, College of Engineering, University of Basrah, Basrah 61001, Iraq

Corresponding Author Email: hussam.jawad.ali@sa-uc.edu.iq

https://doi.org/10.18280/jesa.581208

Received: 2 October 2025
Revised: 10 November 2025
Accepted: 18 November 2025
Available online: 31 December 2025

Keywords:
compound DC motor, series-shunt winding, speed control, PID control, optimization, renewable energy applications, intelligent control

ABSTRACT

In this study, a compound DC motor under different operating conditions is modeled, analyzed, and controlled. Preliminary open-loop simulations at various input voltages revealed limitations, such as slow rise time and steady-state error. Conventional controllers-proportional (P), proportional-integral (PI), and proportional-integral-derivative (PID)-were assessed to control motor speed. A sensitivity analysis, varying key parameters (Ra, J, Ke, and Kt) by ±20%, confirmed the system's robustness and dependence on motor constants. Simulation results showed that the PI controller eliminates steady-state error and speeds up stabilization, the PID controller improves damping and reduces rise time and overshoot, and the P controller enhances transient performance while maintaining steady-state error. By optimizing the PID gains using a grid search approach, the advantages of modern control techniques are demonstrated. This method outperforms conventional PID by achieving faster start-up, less overshoot, and minimal steady-state error. The optimized PID, while maintaining the reference speed at 1500 rpm, provided the quickest start-up and stop times. Among all controllers tested, it delivered the best overall performance, highlighting the critical role of modern control strategies in enhancing DC motor performance and ensuring reliable operation.

1. INTRODUCTION

Combining both series and shunt field windings, the compound direct current motor (CDCM) is a multipurpose electrical device that strikes a compromise between steady speed regulation and strong starting torque [1, 2]. Due to their dual-excitation capability, CDCMs are now widely used in a variety of industrial domains, particularly in electric transportation systems like trolleybuses, where they may also function as generators to facilitate energy recovery and regenerative braking [3, 4]. The use of compound windings improves electromagnetic performance and increases controllability over speed and torque as compared to pure series or shunt motors [5]. Conventional speed control techniques, including shunting the excitation winding to diminish the field, have a number of problems, such as abrupt current surges, nonlinear speed response, and energy losses that lower dynamic stability and efficiency [6, 7]. Advanced power electronic converters, especially DC/DC converters, which enable separate control of the armature and field currents, are used in contemporary methods to overcome these difficulties [8, 9]. Without the surge effects of traditional systems, these technologies allow for continuous speed variation under various load circumstances, enhanced energy economy, and smoother and more accurate speed control [10]. Furthermore, the dynamic responsiveness, resilience to parameter fluctuations, and fault tolerance of CDCMs have been greatly enhanced by recent advancements in control methods, including fuzzy logic controllers, hybrid control techniques, and PID controllers with disturbance observers [11-13]. Because of this, they are ideal for demanding applications such as servo mechanisms and electric cars [14]. The development of CDCMs has also been aided by design advancements. While preserving the benefits of compound excitation, the combination of permanent magnets with brushless topologies improves torque density, decreases electromagnetic losses, and lessens mechanical wear [15]. Moreover, deep learning methods like convolutional neural networks have demonstrated potential in early defect identification and isolation using fault diagnostic methodologies that combine vibration and current signature analysis [16]. These developments increase motor lifespan, decrease downtime, and improve dependability. Overall, advancements in design, control, modeling, and fault diagnostics attest to compound DC motors' ongoing significance. CDCMs continue to be excellent contenders for next-generation electric drive systems and environmentally friendly mobility solutions by fusing traditional motor principles with cutting-edge power electronics and clever control techniques.

2. LITERATURE REVIEW (REVISED FOR COMPOUND DC MOTORS)

A composite least squares method for real-time parameter detection of compound DC motors was presented by Li and Ma [2]. The technique enables quicker and more precise monitoring of motor parameters under varied speed settings by successfully resolving the instability problems related to the conventional forgetting factor least squares. In real-world applications, this development makes it easier to regulate and monitor CDCMs. Soressi [4] investigated the modernization of conventional compound DC motor systems, particularly in industrial lifting and traction applications, building on Li's work. The study suggests using static DC converters in place of antiquated supply methods to improve speed responsiveness and minimize energy losses. Additionally, the paper offers analytical methods for determining motor properties without physically changing the motor's construction. Ludwig [5] concentrated on the transient behavior of compound DC motors during switching and startup operations after advancements in system modernization. In order to comprehend problems such as torque oscillation and current surges, the interplay between series and shunt field components was examined. The work contributed to more dependable motor operation under varied loads by offering mathematical formulations for predicting dynamic performance. Singh [6] investigated the integration of flywheels with compound or shunt DC motors in industrial drive systems as an extension of the dynamic performance studies. Transistor-based control was used to manage peak load demands and minimize speed variations. The outcomes demonstrated preliminary techniques for improving mechanical stability and energy efficiency in CDCM-driven devices. The study by Nuca et al. [11] introduced a revolutionary method for series and compound DC motors that builds on previous control techniques by feeding the armature, series, and shunt windings separately, utilizing different DC/DC converters. Smoother and more energy-efficient speed variation was made possible by the method's elimination of the disadvantages of conventional field-weakening techniques, especially for traction systems, such as shock currents and efficiency.

Building on their earlier work, Nuca et al. [15] proposed a control scheme for compound DC motors under field-weakening conditions that utilizes power converters to manage the armature and shunt windings independently. Results from experiments and simulations showed superior performance over conventional approaches, emphasizing higher control flexibility for dynamic applications, decreased current shocks, and increased efficiency.

A comparative study of several control systems for compound DC motors is provided, building on the conclusions and approaches covered in the earlier research. Key variations in methodology, effectiveness, and application are highlighted in this analysis. Based on recent important investigations, a comparative study has been carried out to assess and contrast the efficacy of different control systems used to compound DC motors. Power electronic converters, sliding mode controllers, disturbance observers, and sophisticated fault detection methods are only a few of the methods covered by the chosen references. Control technique, resilience to parameter fluctuations, disturbance rejection, implementation complexity, and application scenarios are some of the key characteristics that are the focus of the comparison. These elements are included in Table 1 to give a concise summary of the status of the field and to draw attention to the benefits and drawbacks of each strategy. The primary characteristics, approaches, benefits, and uses of the major research covered above are compiled in Table 1, which offers a clear comparison summary.

The reviewed studies demonstrate that modern control strategies and power electronics integration in compound DC motors significantly improve speed regulation, energy efficiency, and dynamic performance across industrial and traction applications.

Table 1. Comparative overview of key studies on compound DC motor control and applications

Ref.	Authors and Year	Focus Area	Methodology / Approach	Key Advantages	Application Domain
[2]	Li and Ma, 2020	Real-time parameter identification	Composite least squares algorithm	High stability, fast and accurate tracking	General CDCM control systems
[4]	Soressi, 2012	System modernization for old CDCMs	Static DC converter integration + parameter analysis	Reduced losses, improved response	Lifting, traction systems
[5]	Ludwig, 2009	Transient behaviour during switching	Analytical modelling of field interactions	Prediction of torque/current surges	Industrial motor control
[6]	Singh, 1973	Load fluctuation management	Integration of flywheels with CDCM + power transistor control	Smoother speed, energy savings	Industrial mechanical systems
[11]	Nuca et al., 2014	Speed control via independent winding supply	Separate DC/DC converters for each winding	Reduced shocks, efficient speed regulation	Electric traction
[15]	Nuca et al., 2010	Field weakening control method	Independent shunt/armature excitation using DC/DC converters	Improved dynamic performance, control flexibility	High-performance applications

3. COMPOUND MOTOR CONFIGURATION

Figure 1 shows the equivalent circuits of series, shunt, and compound DC motors, illustrating the different field winding arrangements:

Compound motors vary according to the distribution ratio of current between the shunt and series field windings, including the following types:

- A motor with equal shunt and series excitation, where each field supplies approximately 50% of the ampere-turns.
- A special compound-wound motor where the shunt field supplies 75% of the ampere-turns and the series field supplies 25%.
- A shunt-wound motor with a light series winding to ensure greater stability under weak field conditions, improving motor performance during operation.

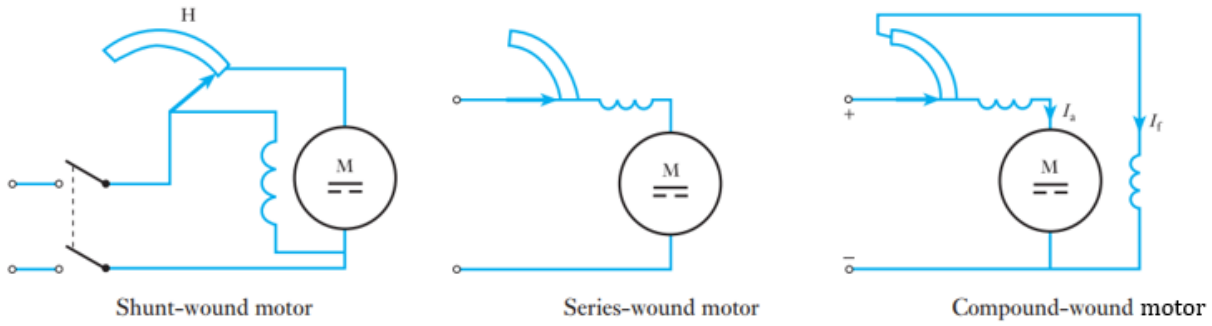

Figure 1. Equivalent circuits of DC motors: Series, shunt, and compound configurations [17, 18]

The shunt field operates at a constant 230 V DC voltage regardless of the armature voltage. Shunt motors can also operate at 460 V, doubling the base speed, with an upper voltage limit of 550 V [4].

In addition to the machine's overall losses, the difference between the motor's input and output power is lost as heat. When producing mechanical power, the motor generates greater temperatures, which cause these losses to increase with load. The field coil and armature windings of a series motor are linked in series with the power source. Numerous twists of heavy-gauge wire are used to wind the field coil. The armature current generates the magnetic field in this kind of motor. When the load is light, the current drawn by the armature is minimal, resulting in a weak magnetic field. Conversely, under heavy load, the armature draws a large current, producing a strong magnetic field. If the little voltage drop in the series field is ignored, the armature voltage is almost identical to the power supply line voltage, much like in a shunt-wound motor. Consequently, a series-wound motor's speed is solely dependent on the load current; under high loads, the speed is low, while at no load it becomes extremely high. If operated without a load, most series motors accelerate to such high speeds that they can destroy themselves, often causing severe damage to surrounding people and property.

Any DC motor's torque is determined by multiplying the armature current by the magnetic field. This connection suggests that when the armature current is high, as it is at start-up, the torque of a series-wound motor is very high [19]. A compound DC motor's torque against armature current characteristic is shown in Figure 2.

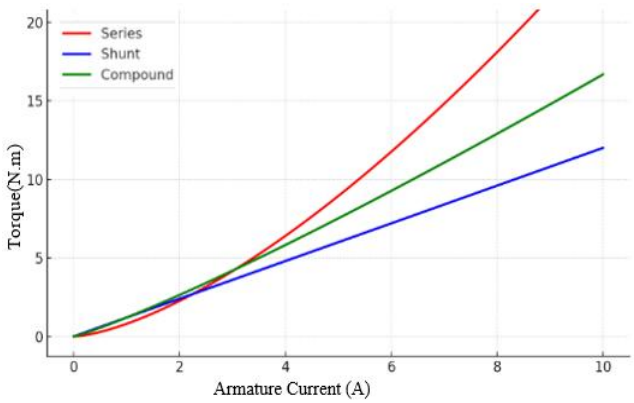

Figure 2. Torque versus armature current characteristics of a compound DC motor

Because of this, a series-wound motor is ideal for powering large, heavy-inertia loads. It is especially suggested for use as a driving motor in electric buses, electric trams, and heavy-duty traction drives. The series DC motor has poor speed management and a large starting torque in comparison to the shunt motor [20].

The operational features of shunt and series motors are combined in a cumulative compound motor. The series-wound DC motor's propensity to overspeed under light loads tempers its high torque capacity. If a shunt field is added and connected to support the series field, this shortcoming can be fixed. Consequently, the motor turns into a cumulative compound machine. Once more, the shunt-wound motor's constant speed characteristic is unsatisfactory in specific situations where DC motors are coupled with flywheels, as it prevents the flywheel from properly dissipating its kinetic energy through a drop in motor speed. A motor with a "drooping" speed curve-that is, one in which the motor speed dramatically decreases as the load increases—is necessary for this kind of application, which is prevalent in punch-press operations. This application is a good fit for the cumulative compound wound DC motor [21].

Applications of cumulative compound motors: This motor is notable for its ability to drastically reduce speed under heavy loads, similar to a series motor, while maintaining a safe peak speed under light loads. As a result, it is utilized:

(i) In situations where beginning requires a lot of torque, and when the load may be abruptly removed.

(ii) In situations when there are significant changes in the load.

Consequently, the ideal applications for compound cumulative motors are in mine hoists, lifts, rolling mills, shearing and punching machines, etc. [22].

The series field can be connected to produce a magnetic field that opposes the shunt field, resulting in a differential compound motor. This type of motor has limited practical application, primarily because it tends to be unstable. The series field is strengthened when the armature current increases in response to an increase in load. But because the shunt winding opposes the series field, the net flow is decreased, which raises the speed. The motor may run away as a result of a feedback loop created by the increasing speed, which can also increase the load. The motor can run safely at no load thanks to the shunt field winding, which effectively restricts the maximum no-load speed. Furthermore, a series coil delivers greater starting torque than a shunt motor, but a shunt coil offers superior speed control. To increase speed control, the series coil can be shorted out after the motor is operating [21].

These motors are used in applications where a comparatively constant speed is required under unbalanced loading conditions. Figures 3(a) and 3(b) illustrate the speed-torque curve versus input current for a compound DC motor [21].

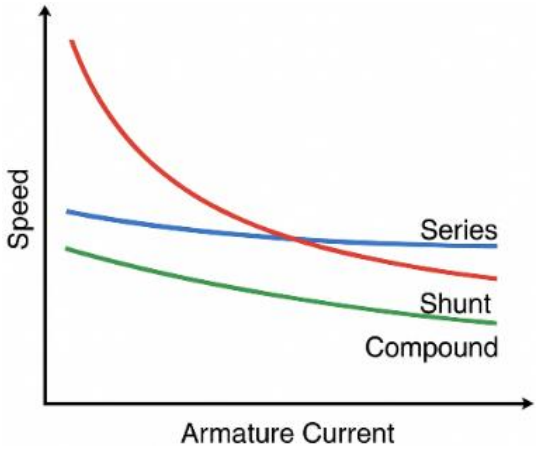

(a)

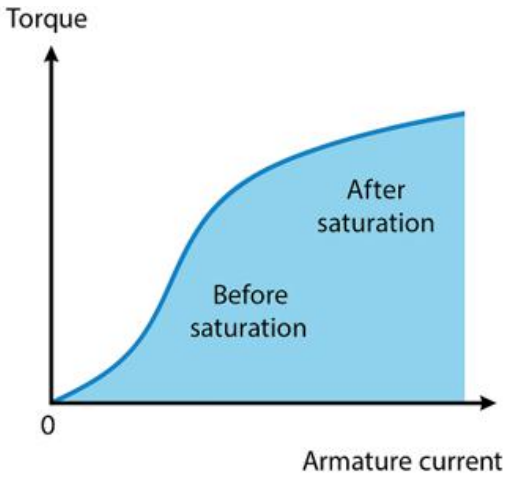

(b)

Figure 3. (a) Motor speed vs. input current; (b) Motor torque vs. input current

4. PERFORMANCE CHARACTERISTICS OF COMPOUND DC MOTORS

Any DC motor's torque is determined by multiplying the armature current by the magnetic field [9]. This equation suggests that for high armature currents, the torque for the series-wound motor will be quite high, as illustrated in Figure 4 [23]:

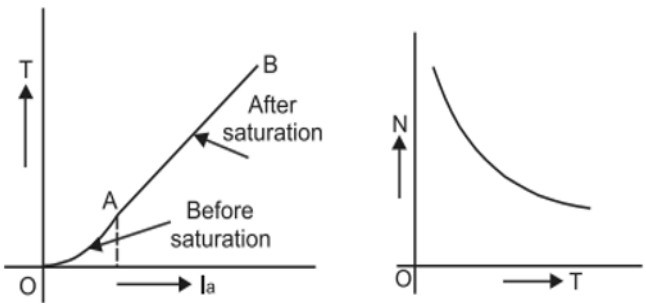

Figure 4. T-Ia & N-T characteristics for a series-wound motor [20]

Figure 5 presents the speed and torque characteristics under load for different DC motor configurations. They include cumulative and differential compound motors, as well as shunt motors, highlighting the variations in performance for each type under varying load conditions.

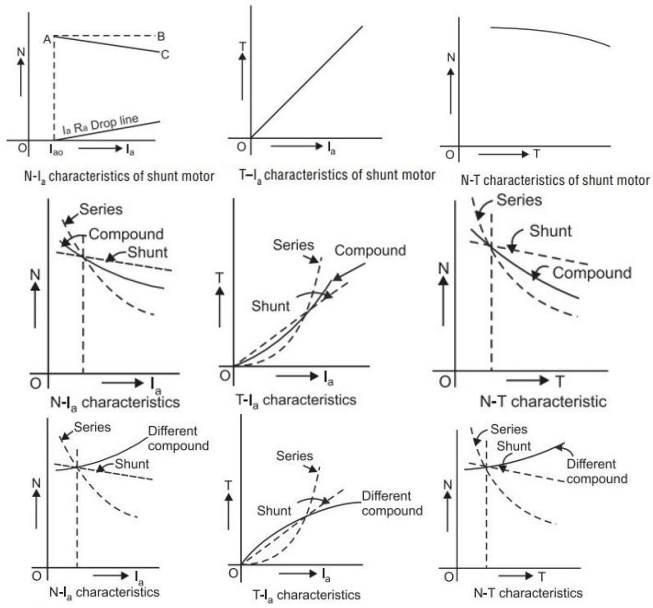

Figure 5. Speed and torque versus load for cumulative and differential compound as well as shunt motors [20]

4.1 Proposed system diagram (system implementation)

A suggested method is created in this work to evaluate and regulate a compound DC motor's (CDCM) performance. The CDCM itself, a transfer function that models the motor dynamics, a step input that represents the reference signal, and the output variables-such as load torque and angular velocity (ω)-make up the system. The general setup of the suggested system is seen in Figure 6, which also demonstrates how each part interacts with the others and how the input signal travels through the system to generate the intended motor response. The motor performance under various load circumstances may be simulated and experimentally validated using this setup's hierarchical framework.

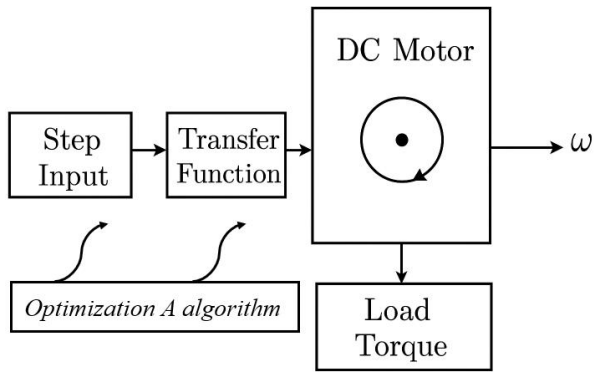

Figure 6. Proposed system diagram for the compound DC motor (CDCM) study, illustrating the step input, transfer function, motor, and output variables including load torque and angular velocity (ω)

4.2 Load characteristics

The connection between torque, armature current, and speed under various load circumstances is described by the load characteristics of compound DC motors. The series component provides strong beginning torque, while the shunt

component stabilizes speed. Torque is determined by the product of armature current and magnetic flux. As the load increases, Figure 4 shows that speed marginally drops, but torque increases with armature current. This illustrates how cumulative compound motors with strong beginning torque and modest speed control may continue to operate steadily. Figure 5 compares the performance of series, shunt, cumulative, and differential compound motors under similar load conditions [20, 22]:

(i) Series motors: very high starting torque with poor speed regulation.

(ii) Shunt motors: nearly constant speed with moderate torque.

(iii) Cumulative compound motors: balance between torque and speed stability.

(iv) Differential compound motors: higher speed under light load but less stable under increasing load.

These characteristics are essential for selecting the appropriate motor type in industrial applications with variable loads, such as electric traction systems or punch presses, where both torque and speed stability are critical for optimal performance [20, 22].

5. MODELLING OF CDCM

Figure 7 shows the matching circuit of a compound DC motor [24]:

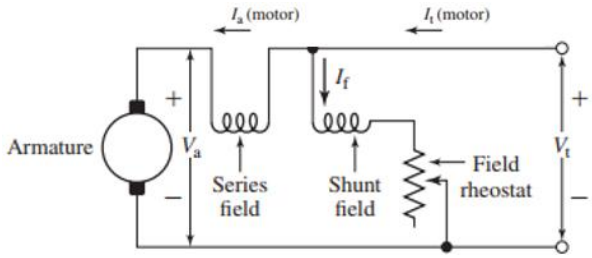

Figure 7. The current directions for a motor or connection schematic: long-shunt connection [22, 25]

The connection diagram in Figure 7 makes the relationships between voltage [25]: Since the shunt voltage is not always equal to the terminal voltage, Eq. (1) shows the total of the series voltage and the armature voltage.

$$V_t = V_a + V_s \tag{1}$$

$$i_a = i_s \tag{2}$$

$$i_t = i_a + i_f \tag{3}$$

The relationship between the armature terminal voltage V_a and the emf E_a produced in the armature of a motor is [25]:

$$V_a = i_a R_a + L_a \frac{di_a}{dt} + b_{emf} \tag{4}$$

$$V_a = i_a R_a + L_a \frac{di_a}{dt} \mp (L_{fm} i_f \mp L_{sm} i_s)\omega \tag{5}$$

$$V_t = i_f R_f + L_f \frac{di_f}{dt} + L_{fm} \frac{di_s}{dt} \tag{6}$$

The motor's generated mechanical power is [4]:

$$P_a = E_a I_a \tag{7}$$

However, the motor torque may be written as follows [4]:

$$T_a = \frac{P_a}{\omega} \tag{8}$$

The following is the relationship between electromagnetic torque and load torque (TL) [24]:

$$T_e = (L_{sm} i_s \mp L_{fm} i_f) i_a \tag{9}$$

$$T_e = J \frac{d\omega}{dt} + B_m \omega + T_L \tag{10}$$

Let $Lsm = Lfm = Lm$ to simplify the model and ignore the word $L_{fm} \frac{di_f}{dt}$. Taking Laplace transform:

$$\omega_m(s) = \frac{\left(L_m I_a(s) \mp L_m I_f(s)\right) I_a(s) - T_L}{JS + B_m} \tag{11}$$

A simulation model of a compound (cumulative) DC motor is developed using MATLAB R-2020a to investigate the motor's performance characteristics and dynamic responses. Figure 8 illustrates the motor's internal structure as a generic block diagram of its interaction between the mechanical and electrical subsystems. Following the derivation of the governing equations of the motor, a mathematical model is constructed, which serves as the starting point for implementing and simulating the motor behavior under varying load conditions. A model of a long shunt compound DC motor built with Simulink transfer function blocks is shown in Figure 8.

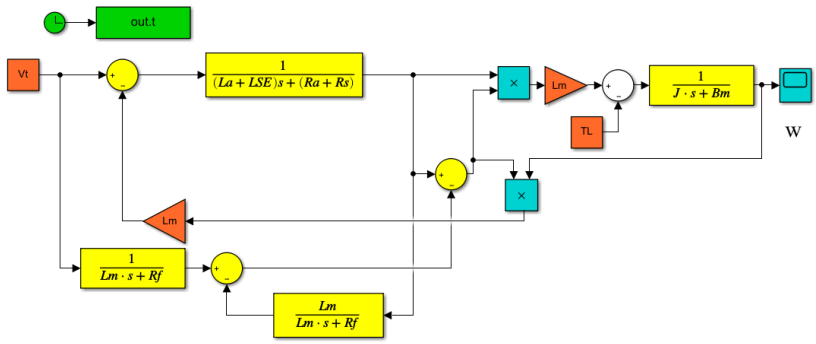

Figure 8. A model of a long shunt compound DC motor using transfer function blocks in Simulink

6. RESULTS AND DISCUSSION

Open-loop tests were conducted at different supply voltages ranging from 24 V to 250 V, and the corresponding dynamic responses were measured. In MATLAB/Simulink, the compound DC motor was modeled using the CDCM model. The combined parameter set, based on Sami et al. [26], was used for the simulation. The motor resistance, inductance, inertia, and viscous friction were taken from the excited motor separately; the shunt field parameters were taken from the shunt-connected motor, and the series field parameters were taken from the series-connected motor. The parameter values used in the cases are shown in Table 2. A sensitivity study was conducted by varying the critical parameters (Ra, J, Kt, Ke) by ± 20% to investigate the effect on the motor speed, current, and torque responses. The summation of these parameters forms the complex current of the motor. The sets of parameters used in this work were originally set for teaching laboratory purposes (Sami et al. [26]). In simulations, a regulated speed of 1500 rpm was selected as a safe and achievable operating point, while open-loop scenarios were tested for supply voltages of 24, 50, 100, 150, 200, and 250 V. As shown in Tables 3-4, the simulated instances of the compound DC motor are given, along with the different supply voltages used to simulate open-loop operation.

Table 2. Parameter specifications for the proposed motor [26]

Parameter	Symbol	Value	Unit
Armature resistance	Ra	0.013	Ω
Armature inductance	La	0.01	H
Shunt field resistance	Rf, sh	1.43	Ω
Shunt field inductance	Lf, sh	0.167	H
Series field resistance	Rf, se	0.7	Ω
Series field inductance	Lf = Lm, se	0.03	H
Mutual inductance	LAF = LSE	0.004	H
Inertia	J	0.21	kg·m²
Viscous friction	Bm	1.074×10^{-6}	N·m·s/rad
Load torque	TL	2.493	N.m
Back-EMF constant	Ke	It is calculated via no-load test = Lm	V·s/rad
Torque constant	Kt	via locked-rotor test or derived from Ke = Lm	N·m/A

Table 3. Compound DC motor simulation cases at various supply voltages

Supply Voltage Vt (V)	Rise Time (s)	Settling Time (s)	Speed ω (rpm)	Notes
24	9.2536	16.0629	75.3620	Stable
50	13.9545	18.6370	266.2054	Stable
100	15.2270	19.0105	665.7735	Stable

Table 4. Compound DC motor simulation cases at various supply voltages

Supply Voltage Vt (V)	Rise Time (s)	Settling Time (s)	Speed ω (rpm)	Notes
150	15.5204	19.0880	1.0721e+03	Stable
200	15.6597	19.1219	1.4793e+03	……
250	15.7303	19.1406	1.8870e+03	……

6.1 Open-loop 24 V - 100 V: For student education

This range is indicative of low-voltage operation for pedagogical use. The open-loop motor speed response at 24 V is examined in this section, as seen in Figure 9. Each step change in voltage was recorded to evaluate the motor speed response, rise time, and settling time, representing the baseline open-loop behavior before higher voltages or controlled operation, as shown in Figure 10.

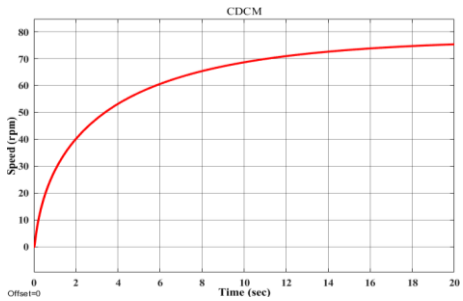

Figure 9. Open-loop motor speed response at 24 V

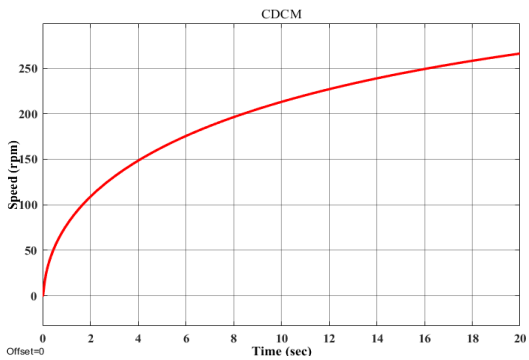

Figure 10. Open-loop motor speed response at 50

Figure 11 shows the open-loop motor speed response at a 100 V supply voltage.

6.2 Open-loop 150 V to 250 V (high-speed range)

Table 4 summarizes the dynamic open-loop performance of the compound DC motor for higher supply voltages (150-250

V). The results include rise time, settling time, and the corresponding steady-state speed, showing a consistent increase in motor speed as the voltage increases while keeping the system behavior stable. Figure 12 shows the motor speed response at 150 V.

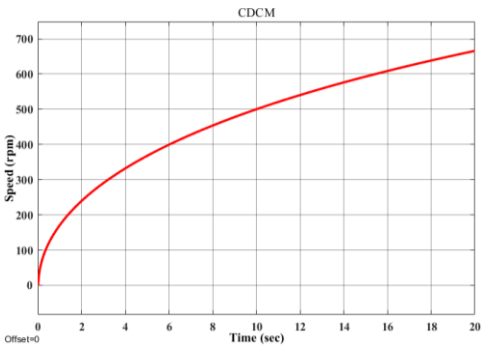

Figure 11. Open-loop motor speed response at 100 V

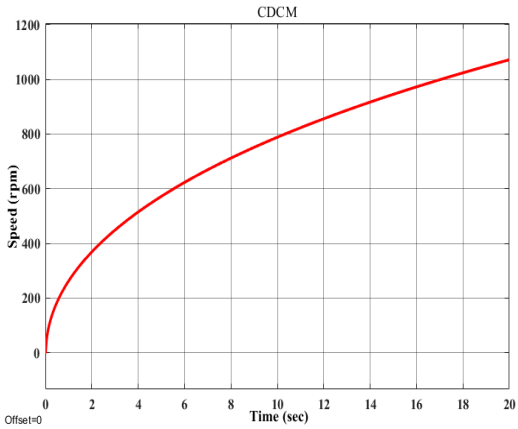

Figure 12. Open-loop motor speed response at 150 V

Figures 13 and 14 display the open-loop motor speed responses at 200 V and 250 V, demonstrating the speed increase as the supply voltage increases while maintaining a stable system behavior.

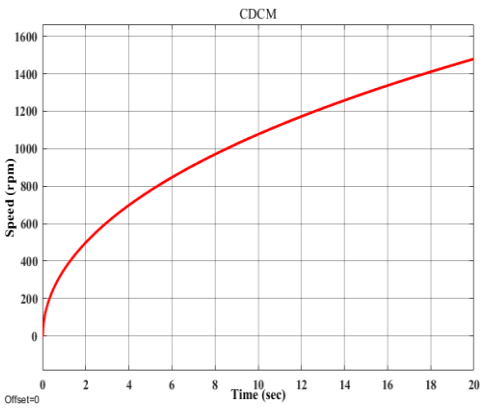

Figure 13. Open-loop motor speed response at 200 V

Figure 15 graphs the motor speed response of the first three supply voltages (24 V, 50 V, and 100 V), all in a single plot. The curves illustrate how the motor begins from rest under increasing voltage levels. Significant points, including rise time, settling time, and peak speed, are indicated using pointers and actual speed values. This graph allows the transient behavior of the motor at lower voltages to be easily compared, with emphasis on the first 20 seconds of operation.

Figure 16 motor speed response for higher supply voltages (150 V, 200 V, 250 V). The graphs show faster acceleration and greater peak speeds. Rise Time, Settling Time, and Peak Speed are marked with corresponding values, allowing for easy comparison of motor operation at higher voltages for the initial 20 seconds.

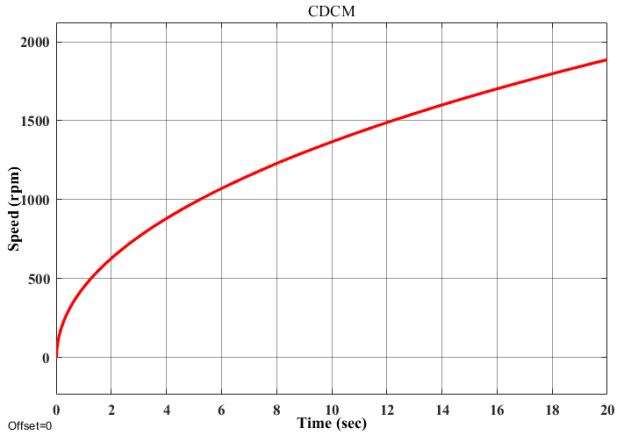

Figure 14. Open-loop motor speed response at 250 V

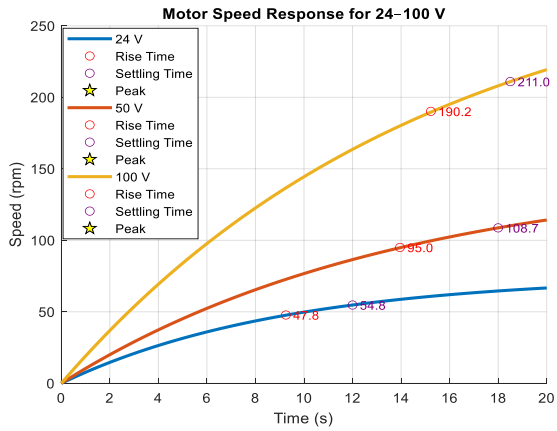

Figure 15. Open-loop motor speed response 24-100 V

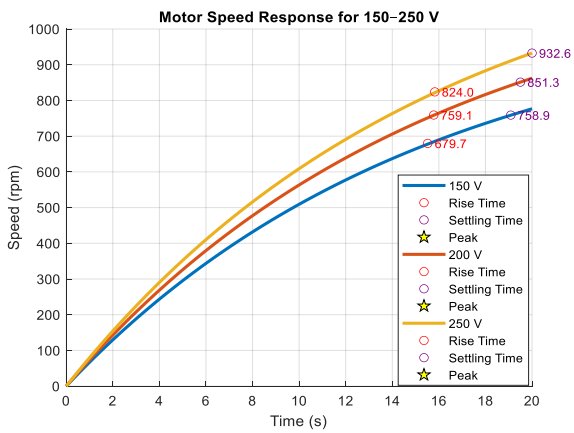

Figure 16. Open-loop motor speed response 150-250 V

Figure 17 indicates the response of motor speed for all six supply voltages (24 V, 50 V, 100 V, 150 V, 200 V, and 250 V) on a single graph. The gradual rise in acceleration and maximum speed with rising supply voltage is indicated by the lines. The subsequent important points, including rise time, settling time, and peak speed, are denoted with respective

values, making a comparison of the transient response over the entire voltage range during the first 20 seconds of operation possible.

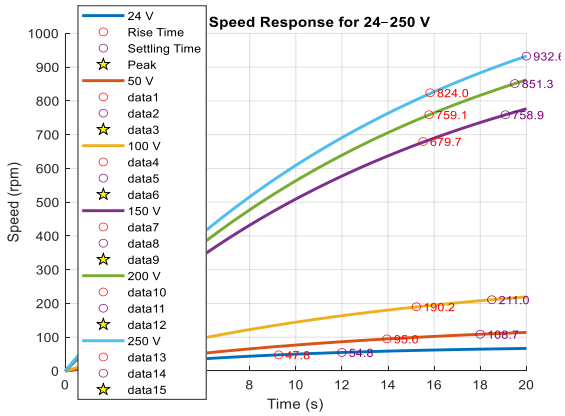

Figure 17. Open-loop motor speed response 150-250 V

A sensitivity analysis was performed by varying the key motor parameters-armature resistance (Ra), rotor inertia (J), torque constant (Kt), and back-EMF constant (Ke)-by ±20% to investigate their impact on motor speed, current, and torque responses. This analysis helps to investigate how these deviations impact the overall dynamic performance because the compounded effect influences the motor's convoluted current and performance. Sensitivity analysis ranges:

Ra: 0.01040 – 0.01560 Ohm

J: 0.168 – 0.252 kg·m^2

Ke: 0.080 – 0.120 V·s/rad

Kt: 0.080 – 0.120 N·m/A

It's worth noting that DC motors come in three basic configurations: parallel, series, and compound. When it comes to the relationship between speed, torque, motor current, and speed, these types behave differently. Figures 18-20 compare the features and illustrate the unique behavior of each configuration for clarity. This comparison focuses on the compound DC motor, which combines the advantages of parallel and series motors and forms the basis for potential control strategies.

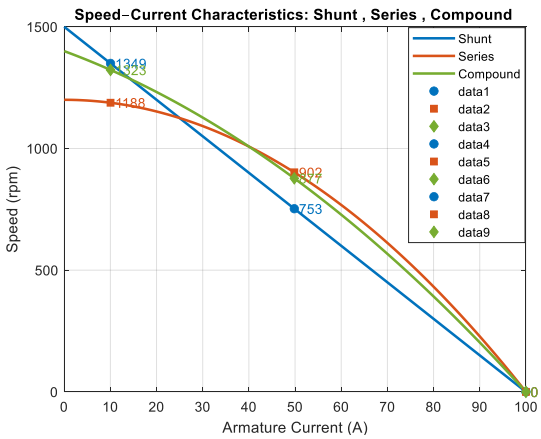

Figure 18. Speed-current characteristics of DC motors (shunt, series, and compound) using illustrative data

6.3 Closed loop

To overcome the limitations of the open-loop response and improve motor speed control, closed-loop control is employed. Figure 21 displays a typical block diagram of the speed control system, with the motor connected to feedback controllers. To assess their effectiveness in sustaining the intended speed, three controllers are used: proportional (P), proportional-integral (PI), and proportional-integral-derivative (PID). Based on the dynamic performance of these controllers in terms of speed response, rising time, settling time, and steady-state behavior, the following conclusions can be drawn.

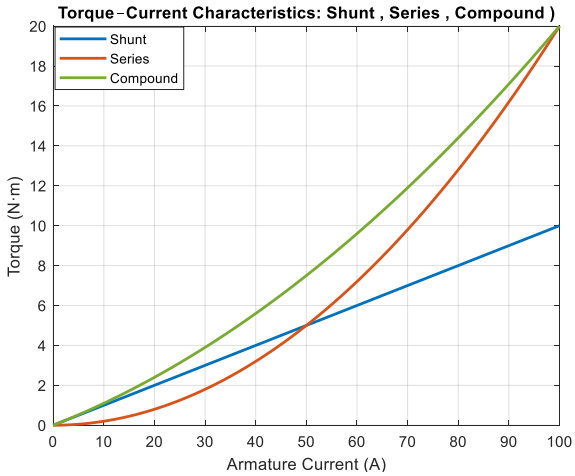

Figure 19. Torque-current characteristics of DC motors (shunt, series, and compound) using illustrative data

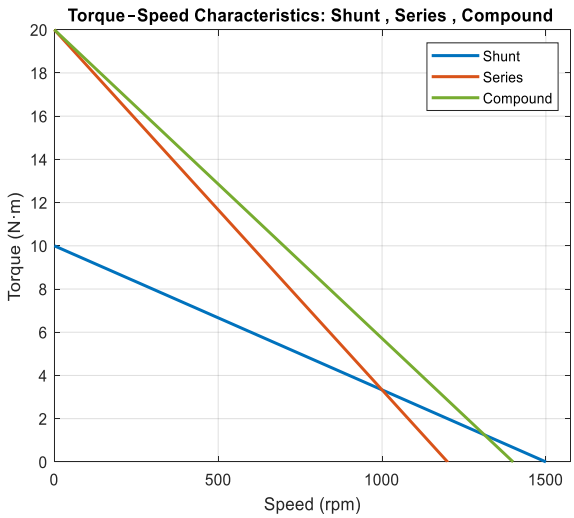

Figure 20. Torque-speed characteristics of DC motors (shunt, series, and compound) using illustrative data

PID controllers used in this study have the following mathematical form [27]:

$$u(t) = K_p.e(t) + K_i \int_0^t e(t)dt + K_d \frac{de(t)}{dt} \qquad (12)$$

where, K_p, K_i *and* K_d the corresponding proportional, integral, and derivative benefits.

u(t) is the control signal. Since it is used to calculate the degree of discrepancy between the intended data input and the actual output value, the input signal of a PID controller (e(t)) is sometimes referred to as the error signal [27].

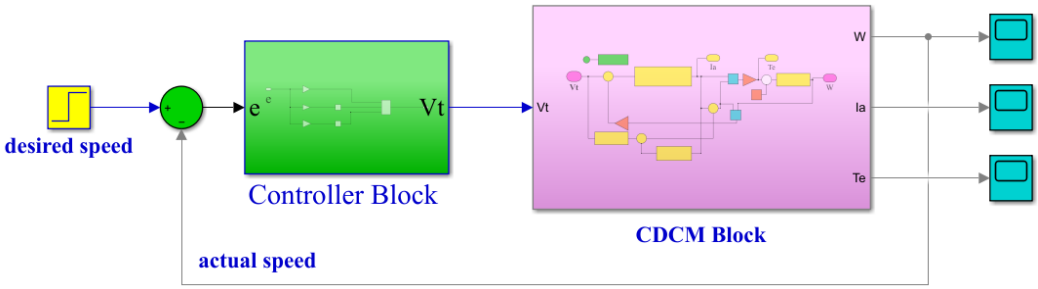

Figure 21. Block diagram for the CDC motor's overall modeling

The motor speed setpoint is the input (setpoint) in a closed-loop speed control system, and the actual motor speed is fed back to the controller. The controller determines the error as the difference between the setpoint and the feedback signal. The controller then processes the error using a PID, PI, or PID controller to generate the corresponding motor voltage, which is applied to the motor terminals. By error-based compensation of the input voltage, the system regulates the motor speed so that the actual speed approaches the desired setpoint with zero steady-state error and good stability. The control process responses suggested by this model are depicted in the figures.

These reactions for various setpoints and control situations are shown in Figures 22 to 25.

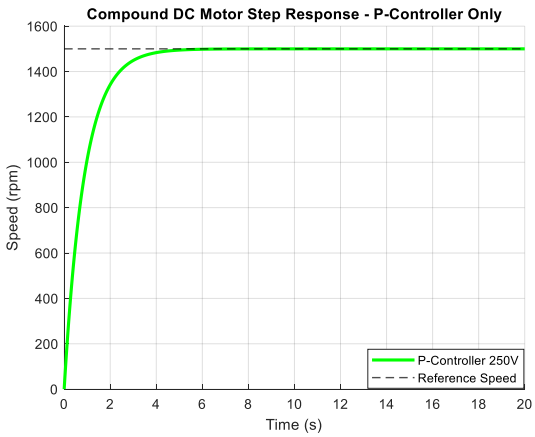

Figure 22. Response of the compound DC motor under the P-controller at 250 V

Compared to the PI and PID controllers, the proportional controller has less accuracy but lowers steady-state error.

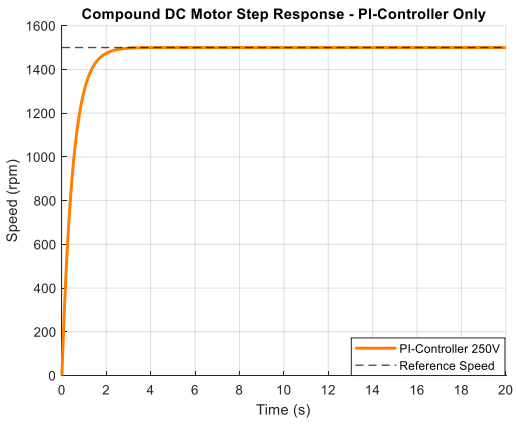

Figure 23. Speed response of the compound DC motor under PI-controller at 250 V

Accuracy is increased and steady-state error is eliminated by the PI action, albeit a longer settling time may be introduced.

With less overshoot, the PID offers an excellent compromise between stability and rise time.

By adjusting the PID gains using the grid-search optimization, a fourth scenario was illustrated in addition to the standard P, PI, and PID controllers. While maintaining the steady-state speed at the reference value of 1500 rpm, the PID controller adjusted (the black plot in Figure 26) and worked better, as seen by quicker rising and settling times. Therefore, out of all the tested controllers, the tweaked PID is the best.

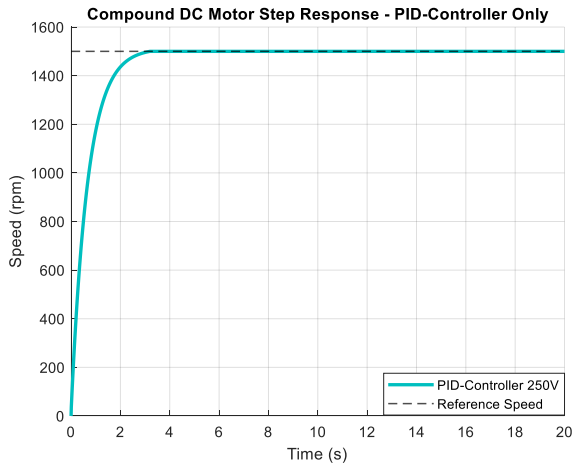

Figure 24. Speed response of the compound DC motor under a conventional PID controller at 250 V

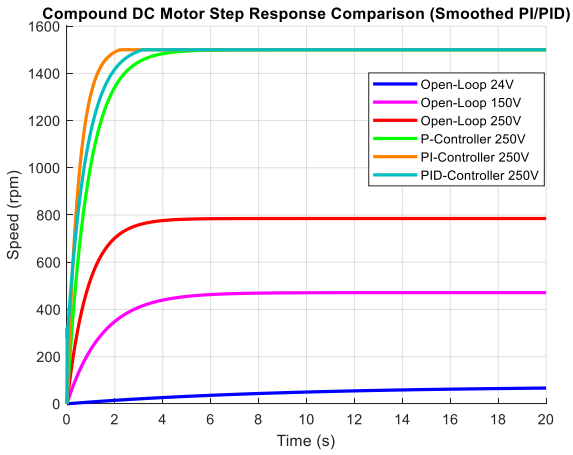

Figure 25. Speed response of the compound DC motor at 250 V under conventional controllers (P, PI, and PID)

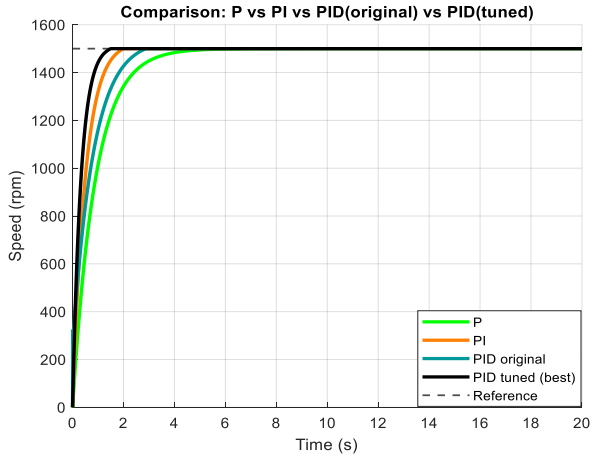

Figure 26. Speed response of the compound DC motor under a tuned PID controller at 250 V

Tables 5 and 6 summarize the performance measures of the four controllers: rise time, settling time, peak value, and steady-state error. These measures will enable a clear quantitative comparison of their dynamic responses.

The performance of the optimized PID controller far exceeds that of the original PID controller. Rise and settling times are lower while the overshoot is eliminated and the steady-state error is reduced from about 45 rpm to about 10 rpm. These results illustrate the strength of the grid-search tuning method and verify that the optimized PID indeed provides a much more accurate and stable speed response for the compound DC motor.

Grid search is a numerical deterministic method widely applied for controller parameter tuning. The method is based on dividing the search space of each parameter into a uniform grid and going through all parameter combinations in their given ranges exhaustively. The performance of the controller in each trial is measured in terms of a cost function or a predetermined performance index, for example, the Integral of Squared Error (ISE), settling time, or maximum overshoot. The optimal set of parameters is selected according to the outcome of the evaluation.

This method is characterized by its simplicity, transparency, and generality to different control systems. However, it has higher computational complexity that grows exponentially with the growth of parameters or search interval sizes, a drawback commonly referred to as the combinatorial explosion. Therefore, in practice, Grid Search is typically employed along with more effective algorithms-e.g., Random Search or Evolutionary Algorithms-to strike a balance between computational effectiveness and search accuracy.

Table 5. The performance values of the four methods

Algorithm	Rise Time (s)	Stelling Time (s)	Peak Val (Rpm)	Steady State Error
P	1.9519	3.4752	1500	1433.7
PI	1.0282	1.6382	1500	1465.5
PID-Original	1.5661	2.3988	1500	1454.9
PID-Grid-Search Optimization	0.69837	1.1565	1500	1489.9

Table 6. The performance values of the four methods

Metric	Original PID	Optimized PID	Improvement
Rise Time (s)	1.5661	0.6984	Faster rise time (≈ 55% improvement)
Settling Time (s)	2.3988	1.1565	Shorter settling time (≈ 52% improvement)
Steady-State Speed (rpm)	1454.9	1489.9	Closer to reference (reduced SSE)
Overshoot (%)	Present (≈ 3%)	0%	Eliminated overshoot completely
Steady-State Error (rpm)	≈ 45.1	≈ 10.1	SSE reduced by ~78%

7. CONCLUSIONS

In this project, open-loop and closed-loop speed control of a compound DC motor using P, PI, and PID controllers was addressed. The open-loop studies have assured that the motor speed is directly proportional to the supply voltage. Safe educational ranges were provided within low voltages (24-100 V), while industrial performance was possible up to 250 V. However, open-loop control has resulted in steady-state error and poor accuracy, which motivates the use of feedback control.

Among the controllers, the proportional (P) controller improved the response but was not able to eliminate the steady-state error. The PI controller successfully removed the steady-state error but exhibited a longer settling time. The conventional PID controller provided a more balanced performance in terms of rise time, overshoot, and steady-state characteristics. The tuned PID controller, represented by the black curve, displayed the best all-around behavior, reaching the set reference speed of 1500 rpm with minimal error, a fast rise time, and a short settling time.

The results obtained from simulations allow recommending the tuned PID controller both for educational laboratory environments and industrial applications involving compound DC motors, since it is characterized by better stability, accuracy, and dynamic response.

Furthermore, the present work can be improved by implementing the proposed control strategies on a real hardware setup to validate the results from simulations. Advanced intelligent control techniques and other optimization methods could further enhance robustness and adaptability for a wider range of motor types.

REFERENCES

[1] Agarwal, K., Mathur, B.L., Sharma, A. (2015). Maximum power transfer to solar powered water pumping system using differential compound DC motor. In 2015 International Conference on Computer, Communication and Control (IC4), Indore, India, pp. 1-5. https://doi.org/10.1109/IC4.2015.7375728

[2] Li, M., Ma, Y. (2020). Parameter identification of DC motor based on compound least square method. In 2020 IEEE 5th Information Technology and Mechatronics Engineering Conference (ITOEC), Chongqing, China, pp. 1107-1111. https://doi.org/10.1109/ITOEC49072.2020.9141652

[3] Oosawa, H., Kimura, G., Shioya, M., Sano, S. (1993). Improved resonant type DC/DC converter for control of a compound DC motor. In Conference Record of the Power Conversion Conference-Yokohama 1993, Yokohama, Japan, pp. 335-340. https://doi.org/10.1109/PCCON.1993.264161

[4] Soressi, E. (2012). New life for old compound DC motors in industrial applications? In 2012 IEEE international conference on power electronics, drives and energy systems (PEDES), Bengaluru, India, pp. 1-6. https://doi.org/10.1109/PEDES.2012.6484440

[5] Ludwig, L.R. (2009). Effect of transient conditions on application of DC. compound motors. Transactions of the American Institute of Electrical Engineers, 47(2): 599-606. https://doi.org/10.1109/T-AIEE.1928.5055020

[6] Singh, V. (2010). Application of power transistor as a slip regulator to DC shunt and compound motors. IEEE Transactions on Industrial Electronics and Control Instrumentation, IECI-20(2): 59-60. https://doi.org/10.1109/TIECI.1973.5408885

[7] Li, K., Chou, F.C., Yen, J.Y. (2017). Real-time, energy-efficient traction allocation strategy for the compound electric propulsion system. IEEE/ASME Transactions on Mechatronics, 22(3): 1371-1380. https://doi.org/10.1109/TMECH.2017.2667725

[8] Yang, J. (2016). Compound controller for DC motor servo system based on inner-loop extended state observer. Cybernetics and Information Technologies, 16(5): 137-145. https://doi.org/10.1515/cait-2016-0060

[9] Morfin, O.A., Castañeda, C.E., Valderrabano-Gonzalez, A., Hernandez-Gonzalez, M., Valenzuela, F.A. (2017). A real-time SOSM super-twisting technique for a compound DC motor velocity controller. Energies, 10(9): 1286. https://doi.org/10.3390/en10091286

[10] Arimitsu, M., Naruse, Y., Minagawa, Y., Nakano, M., Inoue, T. (2005). Characteristics of a coaxial motor driven by compound current (No. 2005-01-3755). SAE Technical Paper. https://doi.org/10.4271/2005-01-3755

[11] Nuca, I., Izmană, I., Eşanu, V., Motroi, A. (2014). Design of separately windings control system of series/compound DC traction motors. Analele Universitatii din Craiova-Seria Inginerie Electrica, 38(1): 189-193. https://ibn.idsi.md/vizualizare_articol/182524.

[12] Shuai, D., Qianfan, Z., Weipan, Z., Chaowei, Z., Tuopu, N. (2019). A compound control strategy for improving the dynamic characteristics of the DC-link voltage for the PMSM drive system based on the quasi-Z-source inverter. IEEE Access, 7: 151929-151938. https://doi.org/10.1109/ACCESS.2019.2948189

[13] Gong, X., Zhi, Z., Feng, K., Du, W., Wang, T. (2022). Improved DCNN based on multi-source signals for motor compound fault diagnosis. Machines, 10(4): 277. https://doi.org/10.3390/machines10040277

[14] Zhang, H., Ge, L., Shi, M., Yang, Q. (2014). Research of compound control for DC motor system based on global sliding mode disturbance observer. Mathematical Problems in Engineering, 2014(1): 759147. https://doi.org/10.1155/2014/759147

[15] Nuca, I., Eşanu, V., Rîmbu, I. (2010). A separate excitation control of compound DC motor. Electrical and Power Engineering, 2: 63-66. https://ibn.idsi.md/vizualizare_articol/163392.

[16] Jiang, M., Zhao, K., Wang, W., Niu, S. (2023). A novel brushless PM-assisted DC motor with compound-excited circular winding. Sustainability, 15(18): 13924. https://doi.org/10.3390/su151813924

[17] Hughes, E. (2008). Electrical and Electronic Technology. Pearson Education.

[18] Gerling, D. (2012). Electrical Machines. Mathematical Fundamentals of Machine Topologies. Mathematical Engineering. Heidelberg, Germany: Springer. https://doi.org/10.1007/978-3-642-17584-8

[19] Rahmani-Andebili, M. (2022). Solutions of problems: Compound DC electric motor. In DC Electric Machines, Electromechanical Energy Conversion Principles, and Magnetic Circuit Analysis: Practice Problems, Methods, and Solutions, pp. 175-181. https://doi.org/10.1007/978-3-031-08863-6_20

[20] Sahdev, S.K. (2018). Electrical Machines. Cambridge University Press.

[21] Iqbal, A., Moinoddin, S., Reddy, B.P. (2021). Electrical Machine Fundamentals with Numerical Simulation Using MATLAB/SIMULINK. John Wiley & Sons.

[22] Fitzgerald, A.E., Kingsley, C., Jr., Umans, S.D. (2003). Electric Machinery. McGraw-Hill.

[23] Kandemir Beser, E. (2023). Extended electrical equivalent circuit for modelling compound DC motors. COMPEL-the International Journal for Computation and Mathematics in Electrical and Electronic Engineering, 42(6): 1892-1904. https://doi.org/10.1108/COMPEL-05-2023-018

[24] Ali, H.J., Shary, D.K., Issa, B.A. (2025). Speed control of separately excited DC motor based on intelligent techniques. Mathematical Modelling of Engineering Problems, 12(7): 2427-2436. https://doi.org/10.18280/mmep.120721

[25] Umans, S.D. (2014) Fitzgerald & Kingsley's Electric Machinery. New York, NY, USA, McGraw-Hill.

[26] Sami, S.S., Obaid, Z.A., Muhssin, M.T., Hussain, A.N. (2021). Detailed modelling and simulation of different DC motor types for research and educational purposes. International Journal of Power Electronics and Drive Systems (IJPEDS), 12(2): 703-714. https://doi.org/10.11591/ijpeds.v12.i2.pp703-714

[27] Ali, H.J., Shary, D.K., Abbood, H.D. (2024). A review of intelligent techniques based speed control of brushless DC motor (BLDC). Basrah Journal for Engineering Sciences, 24(1): 109-119. https://doi.org/10.33971/bjes.24.1.12

NOMENCLATURE

Bm	Damping coefficient, Ns/rad./sec
E	Electromagnetic force, V
i	Current, A
j	Inertia, Kg.m^2
K	Constant
L	Inductance, H
R	Resistance, Ω
T	Torque, N.m
V	Voltage, V

$Kt=kv=Lm$	Torque &back emf constant

Greek symbols

ω	Speed, rad./sec

Subscripts

a	Armature
b	Back
D	Derivative
e	Electromagnetic